Diyala Journal for Pure Science

Study of Aluminum Doping Effect on Some Optical, Structural and Morphological Characteristics of Nanocrystalline Zinc Oxide Films

Rasha Saman Mohammed*, Jasim Mohammed Mansoor ** and Ammer Ayesh Habeeb
Department of Physics – College of Science – University of Diyala

*Jasimmansoor13@gmail.com
**ALzanganawee@sciences.uodiyala.edu.iq

Received: 16 February 2020 **Accepted: 29 September 2020**

DOI: https://dx.doi.org/10.24237/djps.16.04.527C

Abstract

Undoped and Aluminium (Al) doped ZnO thin films with different weight percentages (0, 2, 4, 6, 8%) were deposited on glass substrates using "sol-gel spin coating method". Optical, Crystal structural and surface morphological characteristics of all prepared samples have been studied in terms of their doping effects. The crystal structural analysis was done by X-ray diffraction, and the results showed that all prepared films have "polycrystalline hexagonal" type structure with preferred orientation along (002) for all films except for the percentage (4%) where its preferred orientation was (101). The Al doping leads to decrease the crystallite size of ZnO thin films. Other structural properties such as lattice constant, texture coefficient, dislocation density and number of crystalline per unit area for all prepared films have been calculated. (FE-SEM) images results showed that all prepared films were in the range of (10-100nm) scale nanostructure. Also, the values of average grain size decrease and the surfaces became more homogenous with increase of Al doping ratio. The optical results showed that the optical transmittance is >90%, while the optical energy gap increased with increase of Al doping ratio.

Keywords: ZnO thin films, Sol-gel method, Optical properties, FE-SEM, EDS

Diyala Journal for Pure Science

Study of Aluminum Doping Effect on Some Optical, Structural and Morphological Characteristics of Nanocrystalline Zinc Oxide Films

Rasha Saman Mohammed, Jasim Mohammed Mansoor and Ammer Ayesh Habeeb

دراسة تأثير التشويب بالالمنيوم على بعض الخصائص البصرية والتركيبة والمورفولوجية لاغشية اوكسيد الخارصين النانو بلورية

رشا سامان محمد، جاسم محمد منصور و عمار عايش حبيب

جامعة ديالى- كلية العلوم- قسم الفيزياء

الخلاصة

تم ترسيب اغشية أوكسيد الخارصين (ZnO) غير المشوبة والمشوبة بالألمنيوم (Al) بنسب وزنية (0, 2, 4, 6, 8 wt.%) على قواعد زجاجية باستخدام طريقة السائل الهلامي- الطلاء المغزلي. تم دراسة الخصائص البصرية و التراكيب البلورية و مورفولوجية السطح للأغشية المحضرة كافة فضلا عن تأثير التشويب. تم تحليل التركيب البلوري بأستخدام حيود الأشعة السينية (X-ray). واظهرت النتائج ان الأغشية المحضرة كافة لها تركيب متعدد التبلور من النوع السداسي وبأتجاه تفضيلي (002) عدا الغشاء المرسب بنسبة (4%) اذ كان الاتجاه التفضيلي هو (101). ادى التشويب بـ (Al) الى نقص في حجم البلوريات لأغشية (ZnO) وتم حساب معلمات تركيبية أخرى للأغشية المحضرة كافة مثل ثوابت الشبيكة و عامل التشكيل و كثافة الأنخلاعات وعدد البلوريات لوحدة المساحة. وبينت نتائج (FE-SEM) ان الأغشية المحضرة كافة لها تراكيب بلورية ضمن المدى (10-100nm) للمقياس النانوي، وان معدل الحجم الحبيبي يتناقص، والسطح يصبح اكثر تجانس بزيادة نسبة التشويب. وبينت الخصائص البصرية ان النفاذية البصرية (>90%) بينما تزاد فجوة الطاقة بزيادة نسبة التشويب بـ (Al).

الكلمات المفتاحية: اغشية اوكسيد الخارصين الرقيقة، طريقة السائل الهلامي، الخواص البصرية، (FE-SEM)، (EDS)

Introduction

As a II-VI semiconductor with a wide and direct band gap, ZnO is known for its high chemical and thermal stability, and nontoxic nature. ZnO has drawn great attention in the past few years owing to its enormous significance in optoelectronic and transparent electronic devices [1,2]. ZnO can be doped with a wide variety of ions to comply with the requirements of several fields of application. Due to its high-quality samples with increased band gap, good optical transmittance and higher conductivity, Al is regarded as an efficient n-type dopant, among

others [3]. Al doped ZnO (AZO) is deemed as an ideal prospect for transparent conductive oxide (TCO) due to its properties. Al doped ZnO is also widely applied in optoelectronic devices because of its high optical transmittance in visible wavelength range [4,5]. Also, thin film of Al:ZnO can be used in the photoconductive sensor applications such as UV sensors [6]. Many different methods have been used for synthesis of Al: ZnO films like "radio frequency (RF) magnetron sputtering, spray pyrolysis, electrochemical deposition and sol-gel" processes. Sol-gel grabs more attentions for synthesizing different types thin films because of its wide advantages [7]. Sol-Gel method can be considered as simple, low cost, large area substrate coating method. In this work, different samples of pure ZnO and aluminum doped ZnO thin films have been prepared by "sol-gel spin coating" process, and their optical, crystal structural and surface morphological characteristics were studied.

Experimental details

Pure and Al doped ZnO films samples with different weight percentages (0, 2, 4, 6, 8%), were deposited on glass substrates using sol-gel spin coating method. Zinc acetate dihydrate $Zn(CH_3COO)_2.2H_2O$, aluminum nitrate nonahydrate $Al(NO_3)_3.9H_2O$, 2-methoxy, and monoethanolamine (MEA) were used as starting, dopant source, solvent, and stabilizing agent materials, respectively. The starting zinc acetate, and dopant aluminum nitrate powders were both dissolved in a mixture of (12ml) of 2-methoxy ethanol and (0.4ml) monoethanolamine (MEA) at room temperature. The concentration of dissolved solutions was (0.5M). In next step, the solutions were treated using a hot plate-magnetic stirrer at (70 ^oC for 90 min) in order to dissolve all materials in solvent. Before deposition, the glass substrates were cleaned using distilled water, and ethanol in an ultrasonic bath for (10 min). All thin films were deposited on cleaned substrates using spin coating at (3000 rpm for 30 s) in air. After that, the samples were treated at (250 ^oC for 10 min) in order to remove all solvent and organic components by evaporation from the films. In the final step, the deposited samples were annealed at (500 ^oC for 1 hour).

Table 1: Some chemical properties of materials used

Materials	Chemical formula	Molar mass g/mol	Product country
Zinc acetate	$(Zn(CH_3COO)_2.2H_2O)$	219.50	India
Aluminum nitrate	$(Al(NO_3)_3.9H_2O)$	375.13	India
2-Methoxyethanol	$C_3H_8O_2$	76.10	India
Monoethanolamine	C_2H_7NO	61.08	China

Results and Discussion

The XRD plots of (ZnO:Al) thin films with different Al doping ratios are shown in figure (1). The XRD plots showed that all the films are polycrystalline hexagonal wurtzite structure (ICDD 36-1451). As Al ratio increased, the intensity of diffraction peaks decreased [8]. This result can be explained by increasing the defect in the ZnO structure because of Al atoms. The favored orientation was determined by calculating the texture coefficient $Tc_{(hkl)}$ using the following equation (1) [9]:

$$Tc_{(hkl)} = \frac{I_{(hkl)}/I_{o(hkl)}}{\frac{1}{N}\Sigma\, I_{(hkl)}/I_{o(hkl)}} \quad (1)$$

Where $I_{(hkl)}$, $I_{o(hkl)}$ and N are the measured intensity, the intensity taken from the ICDD data and the total number of peaks in the experimental pattern, respectively. The values of the texture coefficient for all samples are shown in table (2). The values of $Tc_{(hkl)}>1$ indicate the abundance of crystallites in a given growth direction, while values of $Tc_{(hkl)}<1$ indicate that the films do not have a uniform direction. Calculation of texture coefficient shows that the maximum (Tc) values are (002) for all films, except the film deposited at (4%) where its preferred orientation is (101). This difference in the direction of crystallization is explained by the survival model of the fastest. This model assumes that the nuclei process takes several directions in the early stages of thin films crystallization and then the faster-growing nuclei crystallize in a certain

crystalline direction than the rest of the crystallization directions of other slower-growing nuclei [10]. The crystallite size of all samples was calculated by Scherrer's formula [9]:

$$D = \frac{k\lambda}{\beta \cos\theta} \quad (2)$$

Where D, β, k, λ, and θ are the crystallite size, the full width at half maximum (FWHM) in radian, constant (0.9), the X-ray wavelength, and the Bragg's angle, respectively. The following formula is used for the calculation of the lattice constants (a,,c) describing the hexagonal unit cell [11]:

$$\frac{1}{d^2} = \frac{4}{3}\left(\frac{h^2+hk+k^2}{a^2}\right) + \frac{l^2}{c^2} \quad (3)$$

Where (h, k, l) are the Miller indices, d is the interplanar spacing which is determined by Bragg's equation [12]:

$$n\lambda = 2d\sin\theta \quad (4)$$

The dislocation density (δ) is estimated using the relation [9]:

$$\delta = \frac{1}{D^2} \quad (5)$$

The lattice parameters (a, c), and interplanar spacing (d) values were calculated from XRD data collected according to standard (ICDD card no. 36-145) values (table 3).

The (002) peaks were used to calculate the size of crystallites. As shown in table (2), the increase in the Al-doping amount ratio gives rise to decrease in the average of crystallite size from (25.91 nm to 17.33nm) owing to the replacement of smaller Al atoms at Zn site in the lattice of ZnO [7].

Diyala Journal for Pure Science

Study of Aluminum Doping Effect on Some Optical, Structural and Morphological Characteristics of Nanocrystalline Zinc Oxide Films

Rasha Saman Mohammed, Jasim Mohammed Mansoor and Ammer Ayesh Habeeb

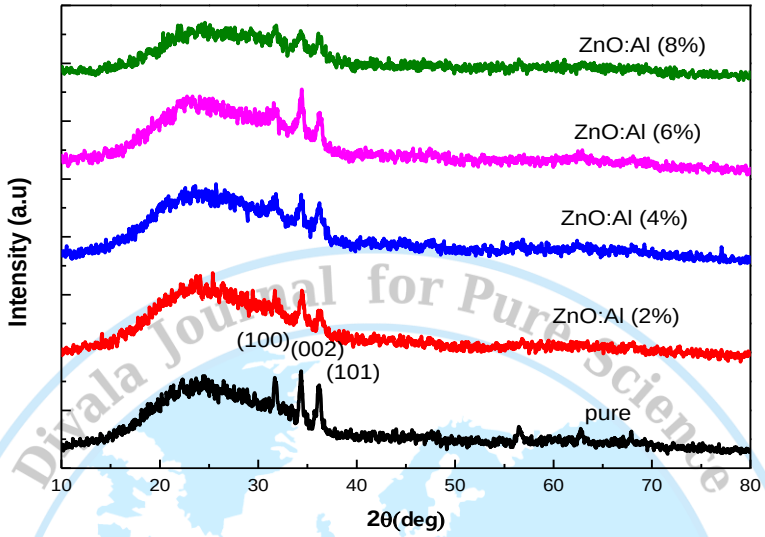

Figure 1: XRD plots of pure and Al doped ZnO films samples

Table 2: The values of the XRD data of pure and Al doped ZnO films.

Sample	2θ(deg)	FWHM	D_{ave}(nm)	$Tc_{(hkl)}$	(hkl)
ZnO Pure	34.3526	0.32170	25.91	1.624	(002)
ZnO:Al (2%)	34.4667	0.59670	13.94	1.813	(002)
ZnO:Al (4%)	36.1968	0.46000	18.17	0.707	(002)
ZnO:Al (6%)	34.3985	0.48000	17.33	1.575	(002)
ZnO:Al (8%)	34.3885	0.42000	19.8	1.382	(002)

Table 3: Structural parameters of pure and Al doped ZnO films samples.

Sample	a (Å)	c (Å)	d_{hkl} (Å)	(hkl)
ZnO (ICDD)	3.250	5.207	2.8143	(100)
			2.6033	(002)
ZnO Pure	3.252	5.216	2.8169	(100)
			2.6089	(002)
ZnO:Al (2%)	3.257	5.200	2.8216	(100)
			2.6006	(002)
ZnO:Al (4%)	3.245	5.215	2.8113	(100)
			2.6094	(002)
ZnO:Al (6%)	3.246	5.210	2.8118	(100)
			2.6058	(002)
ZnO:Al (8%)	3.255	5.211	2.8195	(100)
			2.6067	(002)

Diyala Journal for Pure Science

Study of Aluminum Doping Effect on Some Optical, Structural and Morphological Characteristics of Nanocrystalline Zinc Oxide Films

Rasha Saman Mohammed, Jasim Mohammed Mansoor and Ammer Ayesh Habeeb

The surface morphology analysis of pure and Al doped ZnO films prepared films were studied using field emission scanning electron microscopy (FE-SEM) with (50.00KX) magnification as shown in figure (2). The SEM images showed that the ZnO film grew in the form of semi-spherical nanostructures. These structures are made of a lot of tight grains. The emergence of large size of grains on the surfaces of the ZnO thin film can be clearly observed. Also the SEM images of (ZnO:Al) thin films with different Al doping ratios showed nano-polycrystalline structures, the grain size became smaller when the Al doping ratio to ZnO ratio increased. The spaces between grains of ZnO film became smaller by increasing Al concentration ratio as previously recorded in other reports [13,14].

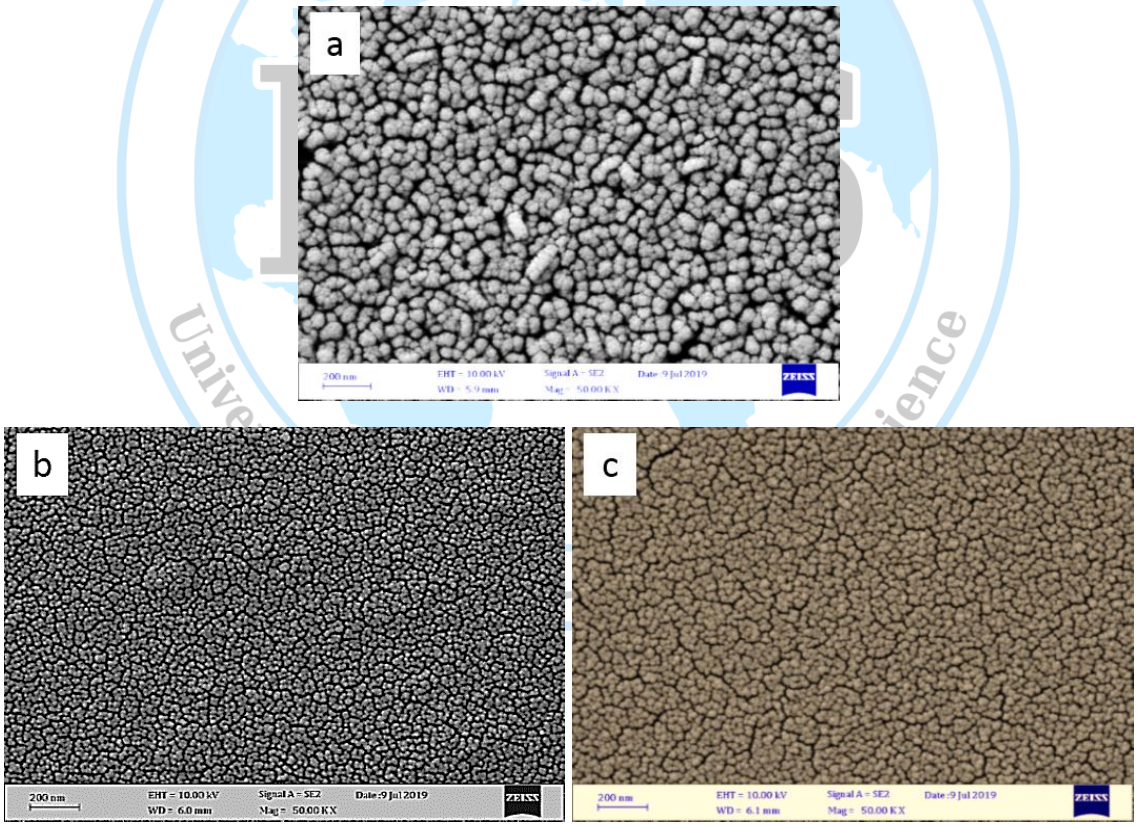

Diyala Journal for Pure Science

Study of Aluminum Doping Effect on Some Optical, Structural and Morphological Characteristics of Nanocrystalline Zinc Oxide Films

Rasha Saman Mohammed, Jasim Mohammed Mansoor and Ammer Ayesh Habeeb

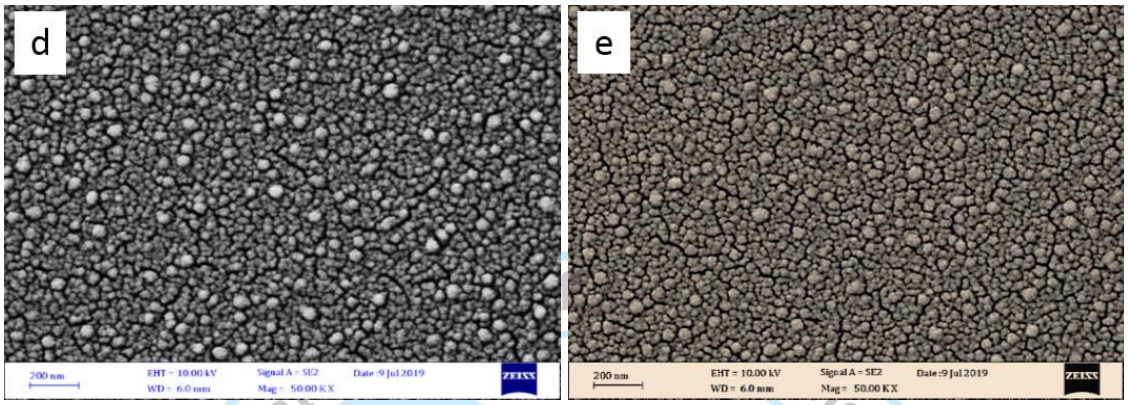

Figure 2: FE-SEM images of pure and Al doped ZnO films samples (a. 0%, b. 2%, c. 4%, d. 6% and e. 8%).

Depending on the FE-SEM images analysis of particle diameters of ZnO thin film and Al doped ZnO films samples with different concentrations of Al, we calculated particles diameters distribution and its histograms for all samples as shown in figure (3). The histogram of diameters distribution of particles of all prepared samples were in the range of nanoscale as shown in table (4). These results showed that the doping of Al to the ZnO thin film leads to decrease the particles diameters distribution of all prepared thin films.

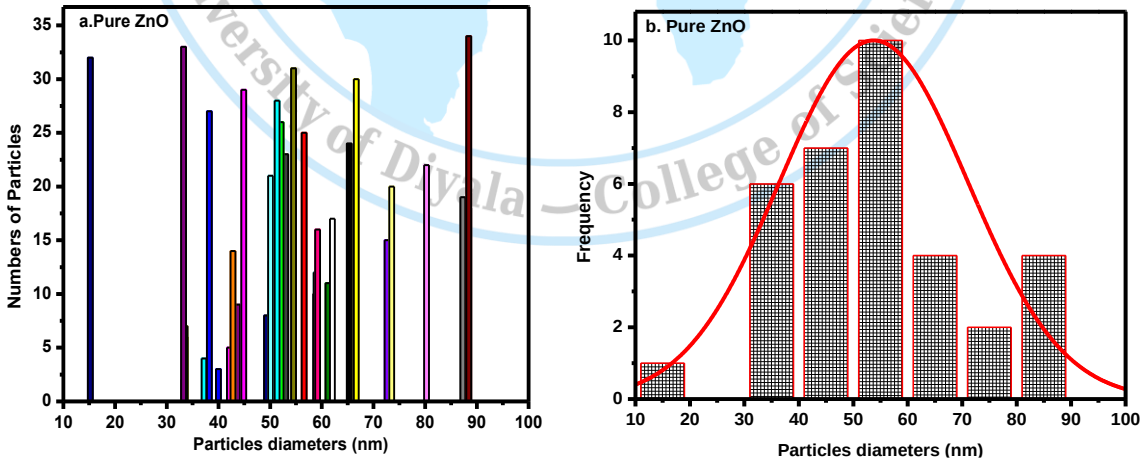

Diyala Journal for Pure Science

Study of Aluminum Doping Effect on Some Optical, Structural and Morphological Characteristics of Nanocrystalline Zinc Oxide Films

Rasha Saman Mohammed, Jasim Mohammed Mansoor and Ammer Ayesh Habeeb

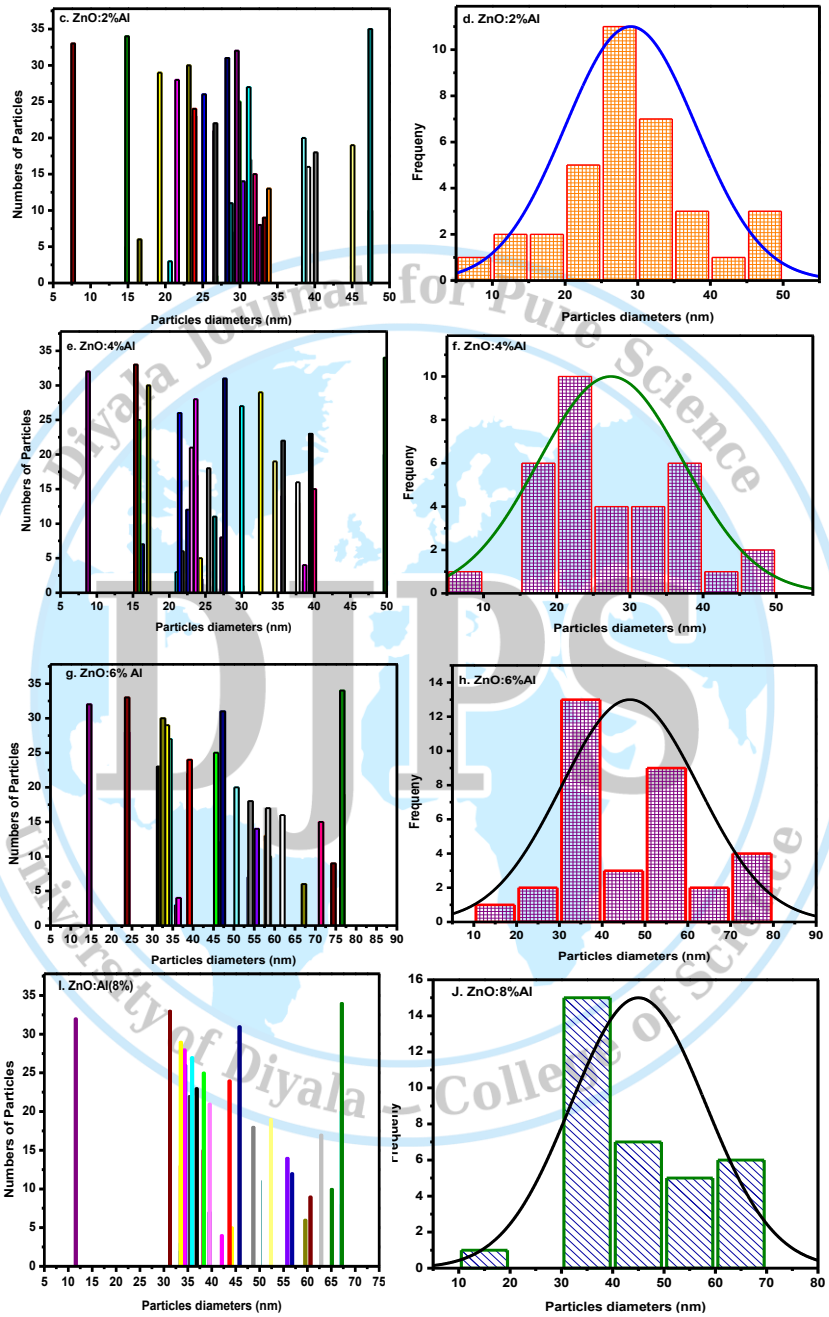

Figure 3: Particles size distribution and its histograms of pure and Al (2, 4, 6, 8wt %) doped ZnO films samples measured using FE-SEM images data.

Table 4: Values of the histogram of diameters distribution of particles of all prepared samples calculated according to FESEM images

Sample	Histogram of diameters distribution of particles range	Histogram of diameters distribution of particles center
ZnO Pure	(10-100nm)	(50-60nm)
ZnO:Al (2%)	(5-50nm)	(25-30nm)
ZnO:Al (4%)	(5-50nm)	(20-35nm)
ZnO:Al (6%)	(10-80nm)	(30-40nm)
ZnO:Al (8%)	(10-70nm)	(30-40nm)

The amount or (concentration) of the elements (Zn, Al, and O) in the prepared thin films samples is examined by (EDS) technique depending on the standard of these elements as shown in figure (4). The peaks of EDS plots of pure and Al doped ZnO films samples showed Zn and O elements in the pure thin films and the Al element doped ZnO thin films. Also the EDS plots showed that all the samples are pure. The EDS results approved preparation of these samples by using Sol-Gel spin coating method.

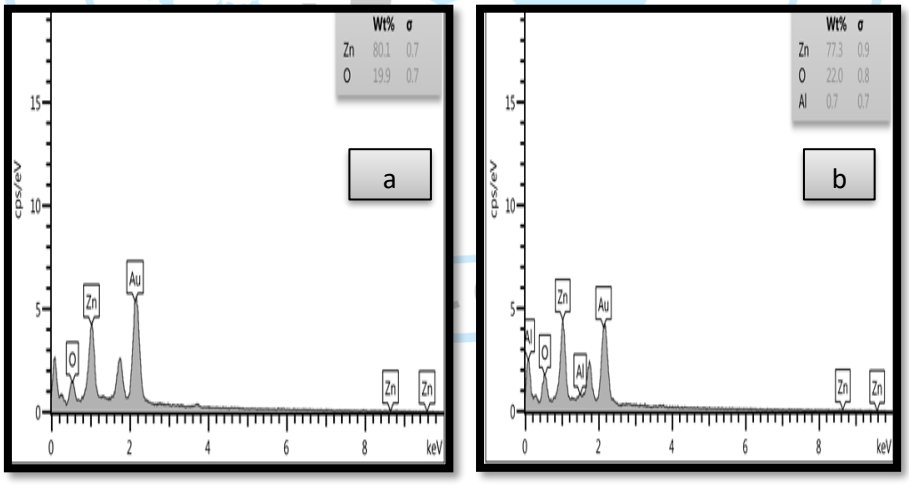

Diyala Journal for Pure Science

Study of Aluminum Doping Effect on Some Optical, Structural and Morphological Characteristics of Nanocrystalline Zinc Oxide Films

Rasha Saman Mohammed, Jasim Mohammed Mansoor and Ammer Ayesh Habeeb

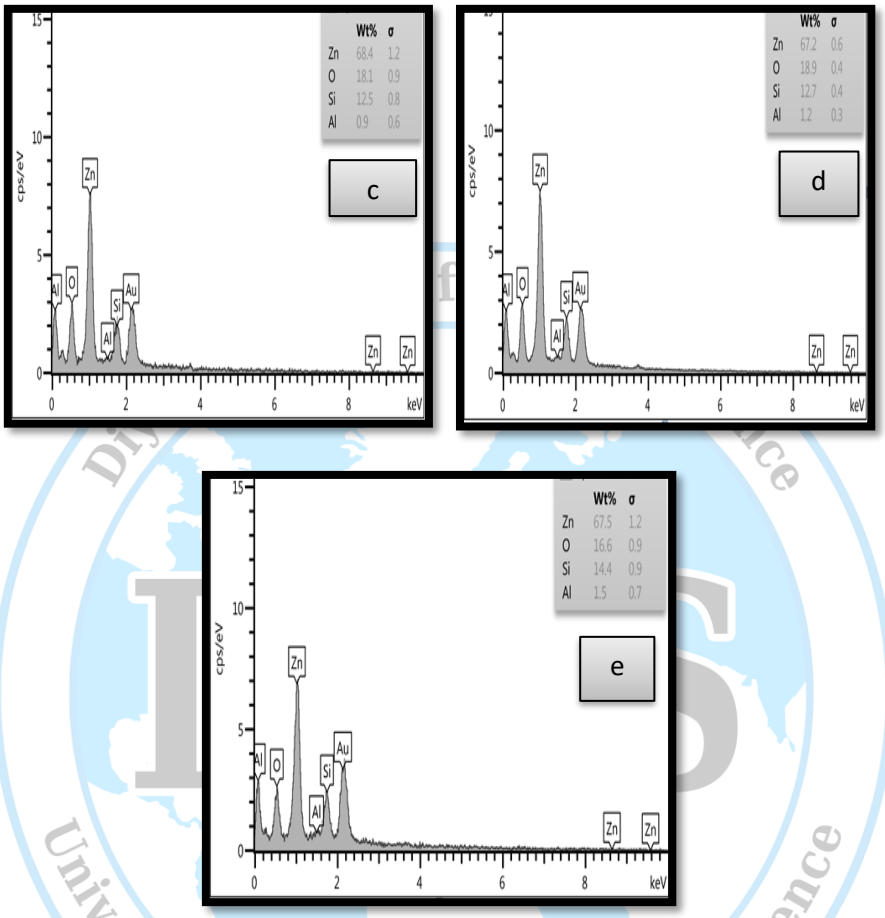

Figure 4: EDS spectra of Al doped ZnO (0, 2, 4, 6, 8wt%) films samples of pure and Al doped ZnO films samples (a. 0%, b. 2%, c. 4%, d. 6% and e. 8%)

The optical measurements of the pure and Al doped ZnO films samples are shown in figures (5) and (6). All optical measurements were done in the (300-900) nm wavelength range at room temperature. All transmittance spectra curves of prepared samples (figure. 5a) showed average transmittance more than 90% in the visible wavelength region. Also, the transmittance spectra curves represent a sharp increase of the films transmittance in the wavelength range from 500 nm to 300 nm. Then, it slows in its increased pace as the wavelength increases. Optical transmittance can be expressed as [15,16]:

$$T=I/I_{\circ} = e^{-\alpha t} \quad (6)$$

Where T, $I_{\circ}$, I, t, and α are the transmittance, incident light intensity on the sample, transmitted light intensity, film thickness, and absorption coefficient, respectively. According to equation (6), the optical transmittance of the thin films decreased by increasing the film thickness. The absorption coefficient (α cm^{-1}) can be calculated from the absorbance (A) using equation [17]:

$$\alpha = (2.303*A)/t \quad (7)$$

Where (t) is the thickness of the film layer. The absorption coefficient (α $(cm)^{-1}$) versus photon energy (hυ (eV)) curves of pure and Al doped ZnO films samples are shown in figure. (5b). From the figure. (5b) in the visible spectrum region, the absorption coefficient of all prepared thin films decreases with the increase of Al ratio. The absorption coefficient values were more than 10^4 cm^{-1} for all prepared samples, indicating that all prepared samples have direct electronic transitions.

In a direct semiconductor of ZnO, the energy gap for allowed direct electron transition is calculated by the following equation [18]:

$$(\alpha h\upsilon)^2 = P\,(h\upsilon - E_g) \quad (8)$$

Where P is a constant for direct transition, and hυ photon energy: Figure (6) shows the relation between $(\alpha h\nu)^2$ and the photon energy (hν). From figure (6), the energy band gap values of all film samples were increased from 3.250 eV to 3.9 eV by increasing of Al ratio. From the literature, the observed blue shift in energy gap can be explained based on the concept of Burstein-Moss effect. The optical band gap is characterized as the minimum energy that an electron needs to jump from the valence to the conduction bands. Thus, the Fermi level is placed in the band gap between the valence and conduction bands. When Al doping ratio increases, free electrons will occupy the lowest states of the conduction band, pushing the fermi level to move towards higher level in energy [19].

Diyala Journal for Pure Science

Study of Aluminum Doping Effect on Some Optical, Structural and Morphological Characteristics of Nanocrystalline Zinc Oxide Films

Rasha Saman Mohammed, Jasim Mohammed Mansoor and Ammer Ayesh Habeeb

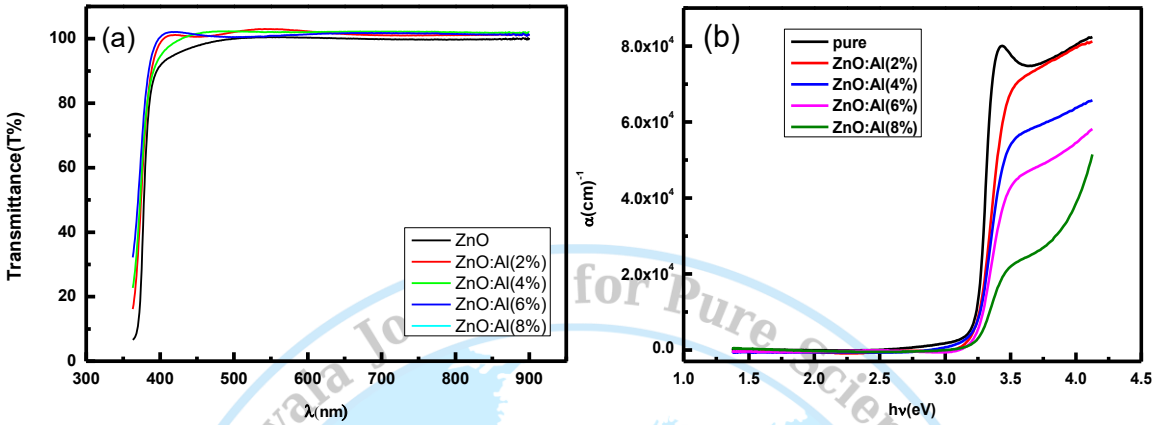

Figure 5: (a) Optical transmittance spectra of pure and Al doped ZnO thin films (b) The absorption coefficient (α cm^{-1}) of the pure and Al doped ZnO thin films

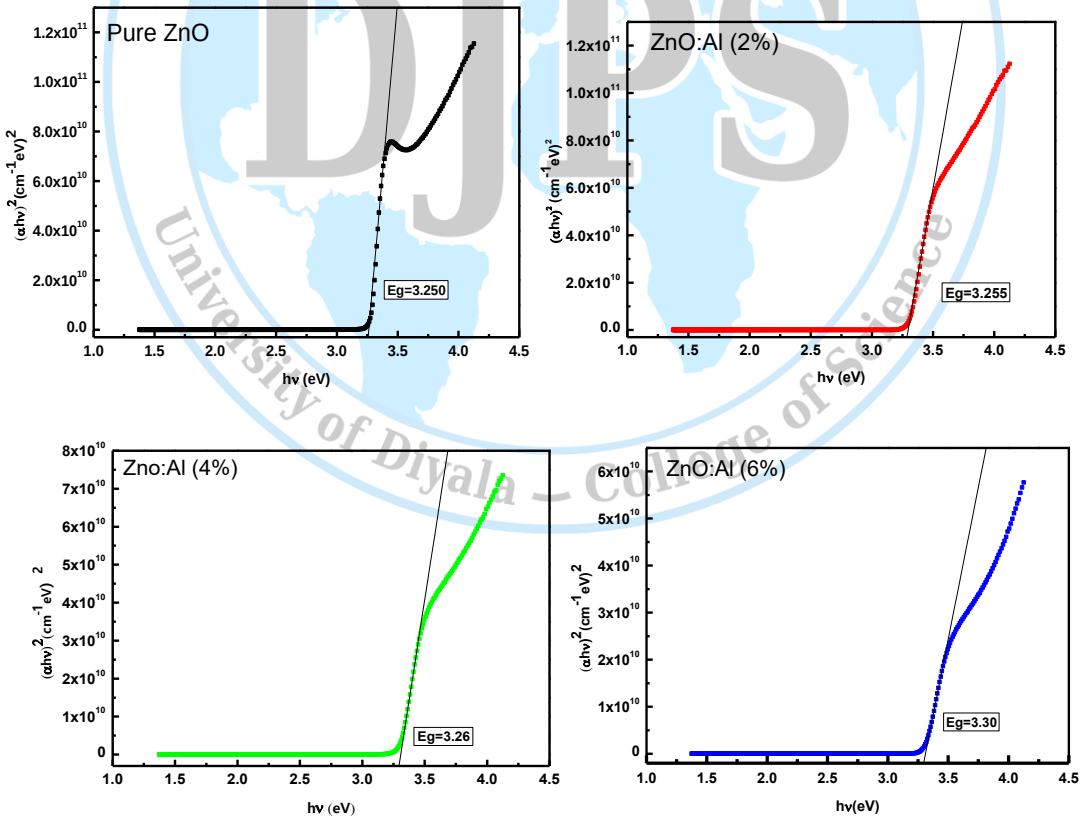

Diyala Journal for Pure Science

Study of Aluminum Doping Effect on Some Optical, Structural and Morphological Characteristics of Nanocrystalline Zinc Oxide Films

Rasha Saman Mohammed, Jasim Mohammed Mansoor and Ammer Ayesh Habeeb

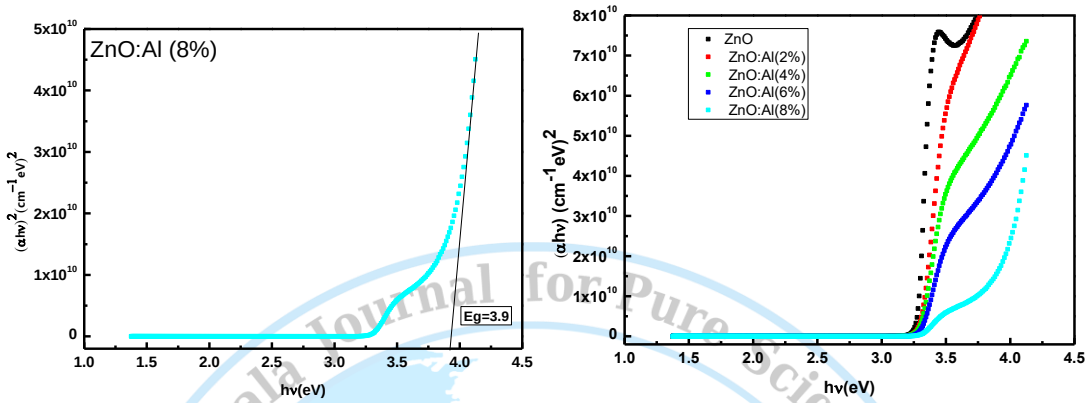

Figure 6: Energy gap of undoped and Al doped ZnO thin films

Conclusion

Al doped ZnO thin films were prepared successfully on glass substrates by sol-gel spin coating method. The structural and optical properties of ZnO thin films have been investigated using XRD, FE-SEM, EDS and UV-Visible spectroscopy. X-ray diffraction (XRD) results showed that all prepared films are polycrystalline hexagonal type structure with preferred orientation along (002) direction for all films except (4%) where its preferred orientation is (101). The size of crystallites was found to be in the range of (25-13nm). The FE-SEM results showed that all prepared films are in the range of nanostructure. The EDS results showed that there are Zn, Al, and O elements in the Al-doped ZnO thin films. The optical results showed that the transmittance and optical energy gap increased with increasing the Al concentration ratio. The shift of absorption edge is associated with Burstein-Moss effect. The transmittance of the films was higher than 90% in the visible region.

References

1. S. Liang, H. Sheng, Y. Liu, Z. Huo, Y. Lu, H. Shen, J Cryst Growth. 225, 110 (2001)
2. W.Yen, Y. Lin, J. H.Ke, Appl Surf Sci. 257, 960 (2010)
3. X. Deng, H. Deng, M. Wei, J. Chen, J Mater Sci Mater Electron. 23, 413 (2012)
4. G. Gordillo, C. Calderon, Solar Energy Materials and solar cells. 69, 251 (2001)
5. P. Nunes, D. Costa, E. Fortunto, R. Martins, Vacuum. 64, 293 (2000)
6. M. Mamat, M. Sahden, Z. Khusaimi, A. Ahmed, S. Abdulah, M. Rusop, Opt Mater. 32, 696 (2010)
7. Y. Caglar, M. Caglar, S. Ilican, Curr Appl phy. 12, 963 (2012)
8. S. Salam, M. Islam, A. Akram, Thin Solid Films. 529, 242 (2013)
9. M. Caglar, Y. Cagler, S. Ilcan, J.Sci. 7, 153 (2006)
10. X. Yu, J. Ma, F.Ji, Y.Wang, X.Zhang, C.Cheng, Journal of Crystal Growth. 274, 477, February (2005)
11. V. Lakshmipriya, B. Natarajan, N. Jeyakumaran and N. Prithivikumaran, Surface Review and Letters. 19, 7, (2012).
12. K. Priya, V. Ashith, G. Roa, G.Sanjeev, Ceram. Int. 43, 10487 (2017)
13. Pogrebnjak, A. Muhammed, E. Karash, N. Gamil, J. Partyka. 4, 315 (2013)
14. W. Lee, J.Young Leem, Journal of the Korean Physical Society. 72, 610 March (2018)
15. O.Stenzxel, The Physics of Thin film Optical Spectra: An Introduction, 2nd ed. (Springer, Publishing Switzerland, (2016), pp.97-98
16. J. Pankove, Optical Processes in semiconductors, 2nd ed, (Dover Publication, 2010), pp 448
17. J. Pippek, semiconductor optoelectronic devices, Academic Press University of California, (2003)
18. Buba, J. Adelabu, The pacific Journal of Science and Technology. 11, 429 (2010)
19. P. Raghu, N. Srinatha, C. Naveen, H. Mahesh, B. Angedi, Journal of Alloys and compounds. 68 (2017)